Available online at www.sciencedirect.com
ScienceDirect
Thermochimica Acta 451 (2006) 1–4
thermochimica acta
www.elsevier.com/locate/tca

Thermodynamic and spectroscopic studies on the phase transition of $BaHf(PO_4)_2$

K. Popa [a,*], R.J.M. Konings [a], O. Beneš [a], T. Geisler [b], A.F. Popa [c]

[a] *European Commission, Joint Research Centre, Institute for Transuranium Elements, P.O. Box 2340, 76125 Karlsruhe, Germany*
[b] *Institut für Mineralogie, Westfälische Wilhelms-Universität, Corrensstr. 24, 48149 Münster, Germany*
[c] *Faculté des Sciences, Université de Nantes, Institut des Matériaux Jean Rouxel, Laboratoire de Chimie des Solides, B.P. 32229, 44322 Nantes Cedex 3, France*

Received 22 June 2006; received in revised form 28 July 2006; accepted 11 August 2006
Available online 30 August 2006

Abstract

We have studied the thermal properties of $BaHf(PO_4)_2$ during the heating from the room temperature up to 1600 K by thermal analysis and drop calorimetry and up to 835 K by Raman spectroscopy. A phase transition appears at about 791 K during heating and at 744 K during cooling. For the high-temperature polymorph we determined the crystal class and the most likely space groups based on Raman spectroscopic data. The enthalpy of the transition was derived from the high-temperature heat capacity measurements.

Keywords: Barium hafnium phosphate; DTA; Ceramics; Phase transition; High-temperature heat capacity; Raman spectroscopy

1. Introduction

The $BaM^{IV}(PO_4)_2$ compounds are interesting for the immobilization of actinides (conditioning), since they can form solid solutions with $M^{III}PO_4$ monazites (M^{III} being a lanthanide or an actinide) of $M^{III}{}_{2-2x}Ba_xM_x{}^{IV}(PO_4)_2$ stoichiometry. The possibility to incorporate neutron absorbers such as Gd on M^{III} sites or Hf on M^{IV} sites is an essential pre-requisite for their suitability as a nuclear waste form. We note here that phosphates containing actinides such as U and Th are known to have a high aqueous durability and a good resistance against self-irradiation [1–5].

A literature survey reveals that all the known $BaM^{IV}(PO_4)_2$ compounds crystallize in the C_12/m_1 space group [6–9] except $BaTh(PO_4)_2$, which exhibits a monoclinic monazite structure ($P2_1/n$ space group) [10] (Fig. 1) or a new, uncharacterised one [12]. The $BaU(PO_4)_2$ compound was not obtained up to date, perhaps because of thermodynamically constraints, since UP_2O_7 forms during the solid-state synthesis. Double phosphates of barium and transuranium elements are not known up to now. On the other hand, $An^{III}{}_{2-2x}Ba_xHf_x(PO_4)_2$ solid solutions containing trivalent actinides could act as nuclear waste form. For example, we have shown in a model inactive study that a single phase $Ce_{2-2x}Ba_xHf_x(PO_4)_2$ monazite-like solid solution forms for $x \leq 0.1$ [13]. A limited miscibility of $BaHf(PO_4)_2$ in $An^{III}PO_4$ (An^{III} = Pu, Am and Cm) is also expected.

For these reasons, we started a systematic study on the thermal stability of the $BaHf(PO_4)_2$ end member. Like $SrZr(PO_4)_2$ [14] and $BaZr(PO_4)_2$ [6,7], $BaHf(PO_4)_2$ also undergoes a first-order phase transition (near 730 K upon heating). Whereas the monoclinic to hexagonal phase transition in $SrZr(PO_4)_2$ is very well defined and occurs at 1196 K [14], the phase transformation in $BaZr(PO_4)_2$ is characterised by the coexistence of the low- and high-temperature polymorph over a temperature range between 750 and 890 K [7,15]. To further characterise the phase transition of $BaHf(PO_4)_2$, the high-temperature behaviour of this compound was studied by differential thermal analysis (DTA), differential scanning calorimetry (DSC), drop calorimetry, and Raman spectroscopy.

2. Experimental

$BaHf(PO_4)_2$ was obtained by solid-state reaction from $BaCO_3$ (Merck), HfO_2 (Alfa Aesar), and $(NH_4)_2HPO_4$ (Merck).

* Corresponding author at: "Al.I. Cuza" University, Department of Inorganic and Analytical Chemistry, 11-Carol I Blvd., 700506 Iasi, Romania.
Tel.: +49 7247 951 448; fax: +49 7247 99670.
E-mail address: karin.popa@ec.europa.eu (K. Popa).

0040-6031/$ – see front matter © 2006 Elsevier B.V. All rights reserved.
doi:10.1016/j.tca.2006.08.011

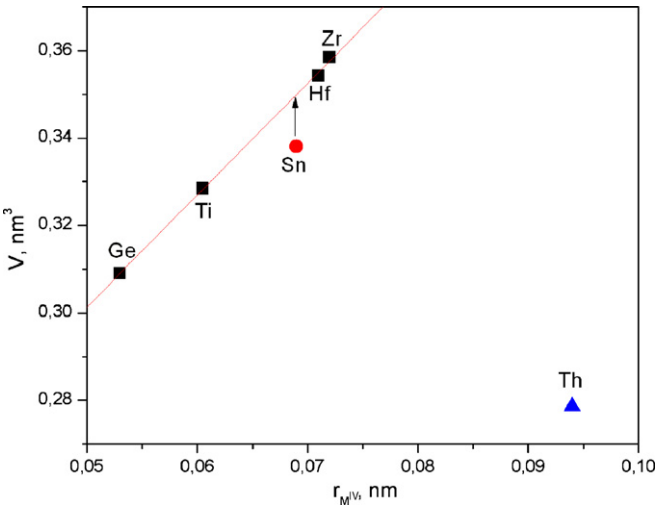

Fig. 1. The cell volume of $BaM^{IV}(PO_4)_2$ as a function of the radii [11] of the M^{IV} cations (into the coordination VI).

The starting compounds were ground in an agate mortar. The reaction mixture was then heated in an alumina crucible at 1523 K for 200 h (with heating and cooling ramps of 100 and 300 K h^{-1}, respectively). An excess of phosphate (25%) was necessary, since unreacted BaO and HfO_2 were detected as impurities in synthesis trials started with equimolar Ba–Hf–P ratios, smaller excess of phosphate at lower temperature, or shorter reaction time.

The sample purity and homogeneity was verified by scanning electron microscopy using a Philips SEM515 instrument with a Tracor northern EDX detector. The compound was further characterised at room temperature by X-ray powder diffraction measurements using a Bragg–Brentano Siemens D5000 diffractometer, equipped with a PSD detector. Cu Kα radiation was used for the measurement. The count step and the dwell time were 0.03° (2θ) and 30 s, respectively. Unit cell parameters were refined on powdered samples by a Rietveld-type method using the Fullprof software.

The thermal behaviour was investigated by differential thermal analysis (Netsch STA 449C Jupiter) in alumina crucibles in an air atmosphere up to 1500 K. The applied heating and cooling rates were 5 K min^{-1}.

The enthalpy increments were determined on parts of ceramic pellets sintered for 5 h at 1673 K using a Setaram multi-detector high-temperature calorimeter (MHTC-96). The measurements were carried out in drop mode, using platinum (99.95% purity) as internal standard in each isothermal run. More details of the technique are described in [16]. A run consisted of up to nine consecutive drops of samples and references, separated by time intervals of about 1200 s during which the heat flux re-stabilised to a constant value. All measurements were performed in air. The relevant reference data for the heat capacity of Pt were taken from [17]. All evaluations of background subtraction and peak integration were done by DSCEval software [18]. A temperature calibration was carried out separately using pure standard metals (Sn, Pb, Al, Ag, and Au) and the reported temperatures have been corrected accordingly.

The heat capacity for the temperature range from 1100 to 1400 K was measured with a Setaram multi-detector high-temperature calorimeter equipped with a DSC detector using the step method. Three sets of measurements were performed to determine the heat capacity of the $BaHf(PO_4)_2$. First the background signal was measured, then the sapphire standard (Al_2O_3) with the known thermodynamic data to obtain the sensitivity of the apparatus, and finally our sample. Each run consisted of 20 steps with a temperature increase of 15 K at the heating rate of 2 K min^{-1}. An isothermal sequence of 4200 s was programmed between these steps to stabilise the heat flow signal. Using this method, it was assumed that the heat capacity during each step is constant and the temperature of each heat capacity point was taken as the average of the start and end temperature of the step.

Raman measurements were conducted with a high-resolution Jobin Yvon HR800 Raman spectrometer using a Nd-YAG (532 nm) laser with ~10 mW power at the surface of the ceramic pellet in the frequency range between 160 and 1300 cm^{-1}. The scattered Raman light was collected in 180° backscattering geometry and dispersed by a grating of 1800 grooves/mm with a spectral resolution of ~1.2 cm^{-1}. A 10× objective with a numerical aperture of 0.75 was used for all measurements. The backscattered Raman signal was collected four times for 15 s. The pellet was heated in a Linkam heating stage for temperature-dependent measurements. The heating and cooling rates between the individual temperature steps were 10 K min^{-1} and the sample was equilibrated for 5 min at the desired temperature. The accuracy of the temperature was better than ±5 K.

3. Results and discussion

The comparison between observed and calculated patterns of barium hafnium phosphate at room temperature is presented in Fig. 2. The cell parameters obtained from the refinement of this structure (space group $C2/m$) are $a = 0.85389(2)$ nm, $b = 0.52928(1)$ nm, $c = 0.78811(2)$ nm and $\beta = 93.170(2)°$. They are in good agreement with those obtained by Paques-Ledent [9] on the basis of the isomorphism with the monoclinic lay-

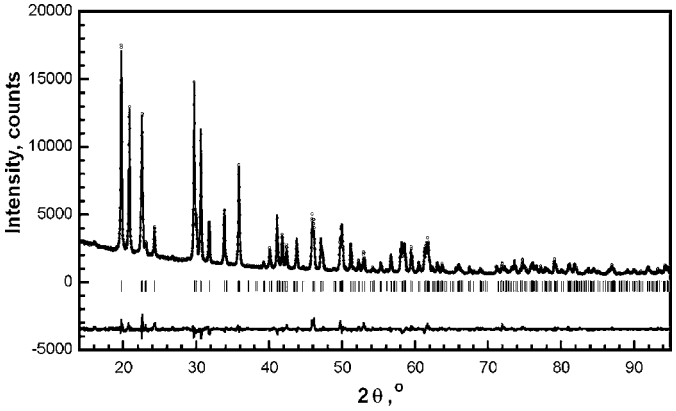

Fig. 2. Room-temperature Rietveld refinement plot of $BaHf(PO_4)_2$, showing the observed (◯), calculated (solid line), and difference pattern (lower). The vertical marks indicate the positions of allowed Bragg reflections.

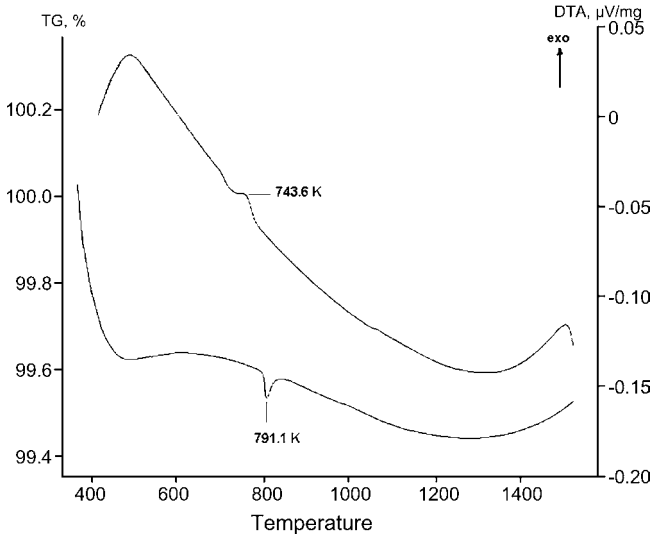

Fig. 3. DTA curve for $BaHf(PO_4)_2$ from room temperature to 1600 K.

ered structure of the yavapaiite $KFe(SO_4)_2$ ($a = 0.8525$ nm, $b = 0.5284$ nm, $c = 0.7874$ nm and $\beta = 93.12°$).

The DTA analysis (Fig. 3) indicates a single event during heating (assigned to a first-order phase transition) at about 791 K (onset temperature). During the cooling, the reverse event was observed around 745 K and only the monoclinic phase was present at the room temperature, as revealed by XRD.

The Raman spectra of $BaHf(PO_4)_2$ recorded from room temperature up to 835 K are shown in Fig. 4. We note that the number of Raman active internal PO_4 vibration modes decrease from nine to six at the phase transition, which was observed around 790 K. The same reduction of Raman bands across the transition has been previously observed for $BaZr(PO_4)_2$ [15]. Group theoretical considerations for the high-temperature polymorph of $BaZr(PO_4)_2$ have shown that the reduction of the number of Raman bands can only be consistent with a trigonal structure, where the Ba and Zr atoms are located at a D_{3d} site, the P and two O at a C_{3v}, and six O atoms at a C_s site in the D_{3d} factor group

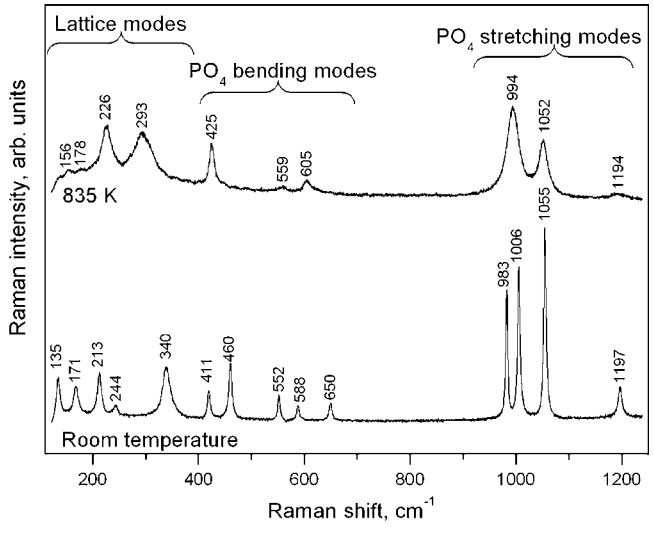

Fig. 4. Raman spectrum from the room temperature and the high-temperature polymorph at 835 K.

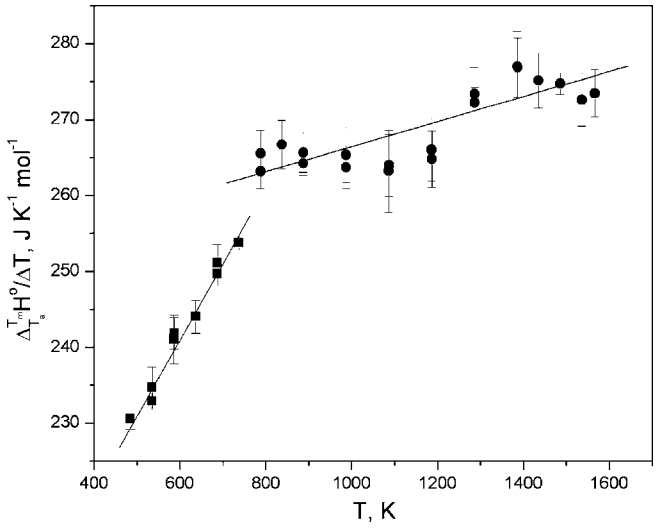

Fig. 5. The reduced enthalpy increment $\Delta_{T_a}^{T_m} H^\circ/\Delta T$ for $BaHf(PO_4)_2$ function of the temperature ($T_a = 298.15$ K).

[15]. Possible space groups for this polymorph were found to be: $D_{3d}^1(P\bar{3}1m)$, $D_{3d}^3(P\bar{3}m1)$ or $D_{3d}^5(R\bar{3}m)$. We conclude here that the high-temperature polymorph of $BaHf(PO_4)_2$ has the same crystal structure as the high-temperature polymorph of $BaZr(PO_4)_2$.

The high-temperature enthalpy increment of $BaHf(PO_4)_2$ was measured from 490 to 1565 K. As shown in Fig. 5, a discontinuity can be deduced from the plot of the reduced enthalpy increment $\Delta_{T_a}^{T_m} H^\circ/\Delta T$, since the results show two distinct groups. It appears between 750 and 785 K and is attributed to the transition between the two modifications of $BaHf(PO_4)_2$ (Supplementary data, Table 1). This is consistent with the Raman and DTA results.

A polynomial fit to the enthalpy increments obtained for the monoclinic phase yielded following equation:

$$\Delta_{T_a}^{T_m} H^\circ\,(\mathrm{J\,mol^{-1}}) = 155.9404\,(T/K) + 95.1856 \times 10^{-3}\,(T/K)^2 - 54955.0 \quad (1)$$

while for the high-temperature polymorph (over 787 K) the fit yielded:

$$\Delta_{T_a}^{T_m} H^\circ\,(\mathrm{J\,mol^{-1}}) = 155.9404\,(T/K) + 95.1856 \times 10^{-3}\,(T/K)^2 - 74977.0 \quad (2)$$

We obtain a transition enthalpy of $\Delta_{trs}H^\circ = 1.71 \pm 0.11$ kJ mol^{-1} ($T_{trs} = 791$ K) from these equations.

Although the enthalpy increment measurements could suggest a second discontinuity between 1200 and 1300 K, no corresponding event was observed by our DTA measurements. Therefore, an additional heat capacity measurement using the DSC detector was performed. The results from the experiment are shown in Fig. 6, where the line represents the result of a

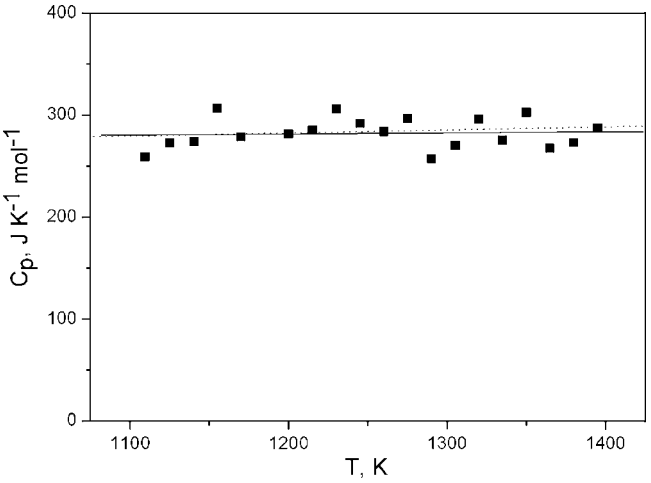

Fig. 6. The heat capacity of $BaHf(PO_4)_2$ between 1100 and 1400 K as measured by DSC. The solid line reflects a fit to the heat capacity data, whereas the dotted line was derived from the enthalpy curve.

regression to the data, which yields following equation:

$$C_p(T)\,(\mathrm{J\,K^{-1}\,mol^{-1}}) = 268.026 + 0.01124\,(T/K)\,(\text{from } 1100 \text{ to } 1400\,\mathrm{K}) \quad (3)$$

The high errors reflect a slight decrease of the sensitivity of the instrument at high temperatures. Nevertheless the data are accurate enough to conclude that there exists no further phase transition. As can be seen in Fig. 6, the heat capacity equations are in excellent agreement with the heat capacity derived by differentiation of the enthalpy curve; the difference is less than one percent.

4. Conclusions

This study revealed the existence of a first-order phase transition during the heating and cooling of $BaHf(PO_4)_2$. This transition was characterised by thermal analyses and Raman spectroscopy. The enthalpy of transition was calculated and the possible space group for the high-temperature polymorph could be restricted to $D^1_{3d}(P\bar{3}1m)$, $D^3_{3d}(P\bar{3}m1)$ or $D^5_{3d}(R\bar{3}m)$. The structure of the high-temperature polymorph has to be further characterised by high-temperature XRD studies. Because of the similarity between the compounds with yavapaiite structure, we predict the existence of similar phase transitions in other $M^{II}M^{IV}(PO_4)_2$ compounds, where M^{II} = Ba, Ra, and M^{IV} = Ti, Zr, Hf, Ge, and Sn.

Acknowledgement

K.P. and O.B. acknowledge the European Commission for support given in the frame of the program "Training and Mobility of Researchers".

Appendix A. Supplementary data

Supplementary data associated with this article can be found, in the online version, at doi:10.1016/j.tca.2006.08.011.

References

[1] R.C. Ewing, W.J. Weber, F.W. Clinard Jr., Prog. Nucl. Energy 29 (1995) 63–127.
[2] A. Meldrum, L.A. Boatner, W.J. Weber, R.C. Ewing, Geochim. Cosmochim. Acta 62 (14) (1998) 2509–2520.
[3] F. Poitrasson, E. Oelkers, J. Schott, J.M. Montel, Geochim. Cosmochim. Acta 68 (10) (2004) 2207–2221.
[4] C. Tamain, A. Özgümüs, N. Dacheux, F. Garrido, L. Thomé, J. Nucl. Mater. 352 (2006) 217–223.
[5] O. Terra, N. Dacheux, F. Audubert, R. Podor, J. Nucl. Mater. 352 (2006) 224–232.
[6] K. Fukuda, A. Moriyama, T. Iwata, J Solid State Chem. 178 (2005) 2144–2151.
[7] K. Popa, R.J.M. Konings, P. Boulet, D. Bouëxière, A.F. Popa, Thermochim. Acta 436 (2005) 51–55.
[8] R. Masse, A. Durif, C. R. Acad. Sci. (Paris) 274 (1972) 1692–1695.
[9] M.Th. Paques-Ledent, J. Inorg. Nucl. Chem. 39 (1977) 11–17.
[10] J.M. Montel, J.L. Devidal, D. Avignant, Chem. Geol. 191 (2002) 89–104.
[11] R.D. Shannon, Acta Crystallogr. A 32 (1976) 751–767.
[12] V. Brandel, N. Dacheux, J. Rousselle, M. Jenet, C. R. Chim. 5 (2002) 599–606.
[13] K. Popa, H. Leiste, T. Wiss, R.J.M. Konings, J. Radioanal. Nucl. Chem., 2007.
[14] K. Fukuda, A. Moriyama, S. Hashimoto, J. Solid State Chem. 177 (2004) 3514–3521.
[15] T. Geisler, K. Popa, R.J.M. Konings, A.F. Popa, J. Solid State Chem. 197 (2006) 1489–1495.
[16] D. Sedmidubský, O. Beneš, R.J.M. Konings, J. Chem. Thermodyn. 37 (2005) 1098–1103.
[17] R. Hultgren, P.D. Desai, T.D. Hawkins, M. Gleister, K.K. Kelly, D.D. Wagman, Selected Values of the Thermodynamic Properties of the Elements, A.S.M., Metal Park, Ohio, 1973.
[18] D. Sedmidubský, DSCEval—software for DSC-data evaluation, Institute of Chemical Technology, Prague, Czech Republic, 2000.